# Power Flow Analysis and Performance Assessment of SST Based Hybrid Distribution System

Gaurav Chauhan[1]*, Sakshi Bangia[2]

[1,2]Department of Electrical Engineering, J.C. Bose University of Science and Technology, YMCA, Faridabad, Haryana, India

**Abstract**

Electricity consumption is rapidly increasing in all the sectors around the world. The most viable solution to the exponential demand of electricity is to encourage the widespread employment of distributed generation (DG) integrating it with a utility distribution system. Numerous advantages of the integrating of DG incorporate system are energy loss reduction, voltage profile augmentation and reliability improvement. In this study, a standard IEEE-14 bus hybrid distribution system has been taken.. The proposed system consists of balanced and unbalanced loads connected to different buses, energy storage system, a solid state transformer based MG, line impedances and it offers the description of necessary data. The model has been analyzed for maximum and minimum demand scenarios and power flow results are discussed for both the cases. The solid state transformer based MG has been proposed and integrated with the existing distribution system and has been analyzed. The thorough analysis of the system provides the potential problems raised and their possible solutions. The proposed system is implemented in MATLAB/simulink environment.

**Keywords**: Renewable energy, Solid state transformer (SST), Hybrid DG, power flow analysis, DC microgrid.

## I. INTRODUCTION

The increased focus on renewable energy sources has significantly led to integration of Distributed Generation with power grid. In addition to other advantages, loss reduction, voltage profile improvement and power flow analysis are its key characteristics. Distributed generation (DG) offers reduced operating costs and establishes flexibility in terms of both investment and installation time. Additionally, renewable energy based DG can have a crucial role in building sustainable energy infrastructure. Typically, distribution systems are structured solely for delivering power to consumers. However, the bi-directional power flow feature alters the characteristics of a distribution network. The bidirectional power flow can also lead to high volatge level if its adoption level is too high. Similarly improper placement and sizing of DG may lead to higher power losses in a system compared to one without DG. Consequently, the

integration of a substantial large amount of Distributed Energy Resources (DER) may cause operational conflicts for a power distribution network.

Currently, the hybrid interconnected network has become more reliable due the incorporation of advance power electronics equipments and development of new micro-processor based technologies. The development in the electrical energy converters and controllers also played significant role in improving system reliability and improves the MG control [1, 2, 3]. Integration of DGs with the main grid not only improves the system reliability but also reduces the investment and construction time. The proper placement of the DG units in active distribution grid significantly decreases the system losses and also recovers the capacity of system to supply loads in real time.

Small interconnected generating systems, which may include RES systems, other generators and energy storage devices at the consumer level to fulfill the demand forms a Micro Grid (MG). MG can be completely AC (i.e. contains all the AC buses which has a benefit to work smoothly along with main grid [16]), DC ( i.e. contain all DC buses) or hybrid of two topologies. Each topology [4, 5, 6] (AC and DC) has its advantages over the other so investigation of HMG may lead to the better power system network [18, 23]. The so far research and actual implementation of MG is shown in [7, 8, 9, 10, 11, 12, 13, 14, 15].

The behavior of MG in a distribution system is generally affected by different factors i.e. the generator characteristics (steady state and dynamic), type of load (linear or non-linear) and energy storage devices dynamics. Sudden unavailability of main grid may also affect the HDG. In any distribution system the hybrid-MG must be tested with distinct conditions i.e. maximum and minimum demand scenarios. Hybrid-MG must be capable of handling abnormal conditions due to load variation. Three level control schemes can be applied for the proper operation and parameter control [17, 30] of MG. The alignment of renewable energy sources and power quality are some other problems faced by MG. The advancement in the power electronics devices and its application in the grid technology [19, 20, 21] enable the smooth interconnection of RES with the grid while a proper implementation of closed loop technique [24, 25, 26] can help in improving the power quality.

In the proposed system three stage topology of SST has been taken which forms two intermediate DC buses i.e. MVDC and LVDC bus. Here the LVDC bus of SST has been utilized for the interconnection of DG and energy storage system. Due to the incorporation of power electronics devices for the purpose of interconnection, it is essential to ensure a proper control of PE devices. In the proposed system, open loop and closed loop control [27] strategies has been implemented for the different converters and PWM techniques at different carrier frequencies are used [28, 29]. The primary aim of the proposed system is to study the behavior of HDG under different operating conditions and to form a micro-grid based on SST and its interconnection with the distribution system.

The proposed system is a hybrid distribution system consist AC as well as DC buses. The distributed resources are interconnected with the existing distribution system at two different voltage levels (MV and LV) which are then feeding to the different types of loads. Improved reliability, reduction in THD, reduction in losses are the vital features of the proposed system. A Solid State Transformer (SST) is employed to form a DC micro grid. The common DC bus of SST is utilized for the interconnection of DG and storage system.

This paper is structured in different sections, section-2 describes the implementation of proposed model and its subsections give the data used for the various component of the proposed model. Section-3 introduces results analysis of power flow study. Section-4 provides the simulation results and discussion for the various cases and section-5 deals with the concluding remarks and the further scope of the study.

## 2. PROPOSED MODEL

The proposed system has been simulated in MATLAB/SIMULINK environment using simscape library. The detailed description of the model is presented in this section. The main purpose is to provide the better understanding of DG interconnected with three phase distribution system and to examine the power flow study and their performances under different operating conditions.

Figure 1 shows the single line diagram of the proposed system. Considering ,grid of 100 MVA is connected to sub transmission system of 69 KV through a PCC. The X/R ratio of main grid is considered to be 10. The proposed distribution system distributes the power at two different voltage levels: the primary distribution level at 13.8 KV and the secondary distribution level which is at 0.22 KV. The outlined system comprises of three sub micro-grids out of which two are AC MGs and one is DC MG hence they together form a hybrid- Distribution system. AC MG1 and AC MG2 are connected together through line 4, 5 and 6. AC MG1 is an area consists of 4 loads to which energy is provided by diesel generator. A PV array combined with energy storage system forms AC MG2 which operates at the frequency of 60 Hz. Also, the third area is DC MG which is linked to the distribution system at bus-2 by the switch-1. The proposed DC MG utilizes the advantage of Solid State Transformer. The SST provides two DC buses at different voltage levels which can be utilize to interconnect renewable sources and local DC loads can also be linked to these DC buses. Apart from that these can be utilize for the purpose of electric vehicle charging. The detailed description of DC MG is explained in the next section.

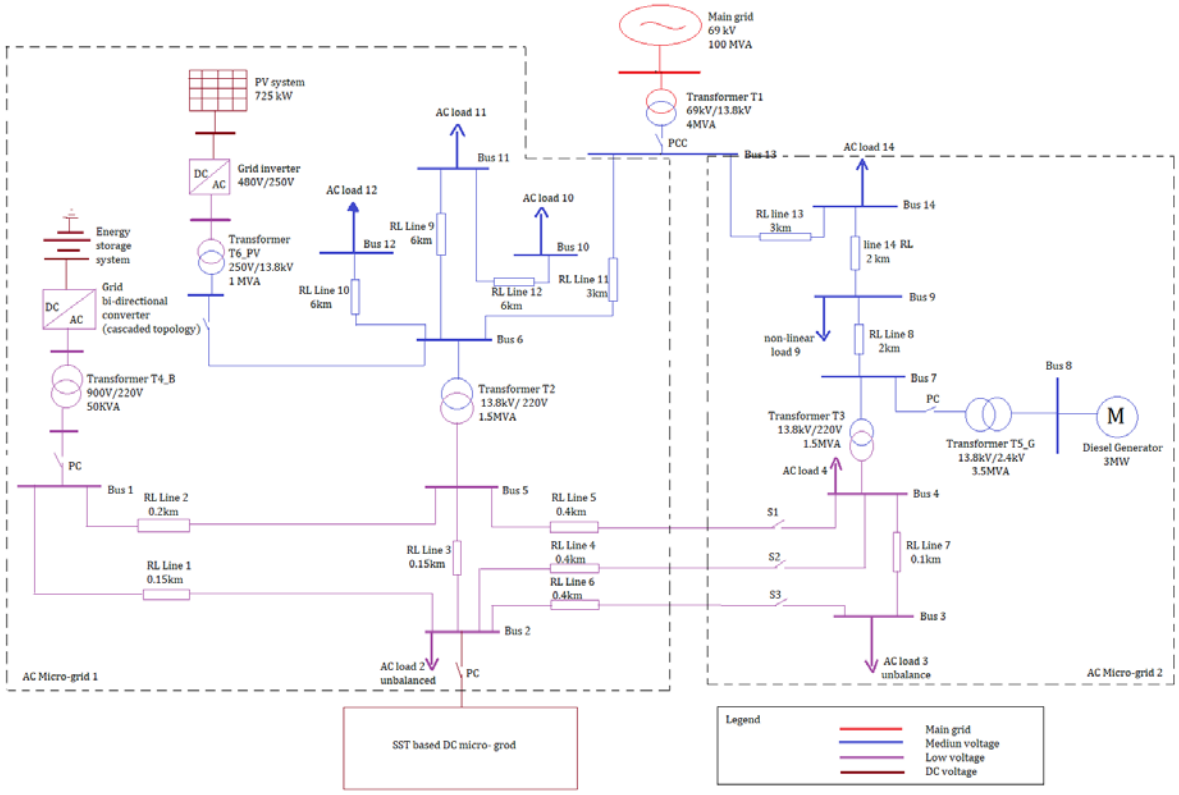


Figure 1: Single line diagram of proposed system

### a. PV Subsystem

The proposed system consists of a photo-voltaic system which forms one of the AC MG linked to the distribution system. The main parameters of the photo-voltaic system for the simulation purpose are mentioned in table 1. The PV array 1 develops a power of 725 KW with the help of 1750 modules. The operating temperature is 25$^{o}$C at an irradiance of 1000 W/m$^{2}$. Uncontrolled circuit of sinusoidal PWM based inverter is used to convert 480 volts DC into 250 volts AC.

Table 1: PV Parameters

| Parameters | Value |
|---|---|
| Current at max power point ($I_{MPP}$) | 5.69 amp |
| Maximum power ($P_{max}$) | 414.8 W |
| Open circuit voltage ($V_{oc}$) | 85.3 V |
| Short circuit current ($I_{sc}$) | 6.09 amp |
| Voltage at max power point ($V_{mpp}$) | 72.9 V |

### b. Battery storage system

Two battery storage energy systems are used: one in the AC MG and other in the DC MG system. The battery energy storage system which is used in the AC MG consists of three-Ni-MH (nickel metal hydride) with the rated capacity of 1.5 Ah and nominal DC voltage of 650 V each. All the tree batteries are connected in parallel and in turn linked to an inverter in a cascaded arrangement. The discharge and charge process of the Ni-MH battery is governed by the following equations:

$$E_{dis\text{-}Ni\text{-}MH} = E_0 - k\frac{Q}{Q-It}i^* - k\frac{Q}{Q-It}It + Exp(t) \quad (1)$$

$$E_{Ch\text{-}Ni\text{-}MH} = E_0 - k\frac{Q}{|It|-0.1Q}i^* - k\frac{Q}{Q-It}It + Exp(t) \quad (2)$$

For $i^* > 0$ ; discharge condition

And $i^* < 0$ ; charge condition.

Similarly, the charging and discharging equations of lithium-ion battery are given by

$$E_{dis\text{-}Li\text{-}Ion} = E_0 - k\frac{Q}{Q-It}i^* - k\frac{Q}{Q-It}It + AExp(-Bit) \quad (3)$$

$$E_{Ch\text{-}Li\text{-}Ion} = E_0 - k\frac{Q}{|It|-0.1Q}i^* - k\frac{Q}{Q-It}It + AExp(-Bit) \quad (4)$$

Where

$E_0$ = constant voltage of battery

K = polarization constant in Ah-1

Exp(t) = exponential zone dynamics in V.

Q = maximum capacity of the battery in Ah

$i^*$ = filtered low freq current dynamics in A

A = exponential voltage (V)

B = exponential capacity ($Ah^{-1}$)

### c. Voltage source converter (DC-AC)

The photo-voltaic system1 is linked to HV distribution system using an inverter through a distribution transformer, which forms an interconnection between AC side of inverter and distribution grid. A three-level IGBT bridge incorporated with PWM control technique is used for

the converter modeling, which converts 480 volts DC to 250 volts AC. The carrier frequency of the PWM is considered to be 2 K Hz, which is operating at closed loop control strategy.

A battery operated energy storage system is also linked to the LV distribution system through an inverter; the inverter boosts the voltage from 650 volts DC to 900 volts AC. A distribution transformer is also used to form an interconnection between the AC side of inverter and the low voltage distribution grid. The major concern while choosing the inverter topology is with power losses, THD and efficiency. Keeping the above mentioned concerns in mind a cascade h-bridge multilevel topology is used, which is considered to be most reliable and efficient.

The state of battery i.e. charging or discharging will depend upon the modulation index and the different scenario (i.e. maximum demand or minimum demand) in which system is operating. In case of maximum demand the battery will discharge through converter using an over modulation-index of 1.2, while in case of minimum demand battery will charge with an under modulation index of 0.8 used by converter.

### d. Power Transformers

The proposed system utilizes a total of 7 power transformers in the study. A substation transformer of 69/13.8 kV rating is used to form an interconnection between the 1000 MVA utility grid and 13.8 KV high voltage distribution system. Distribution transformer T2 and T3 forms the interconnection between HV distribution system and LV distribution system. Remaining transformers are used to interconnect storage system and rest of the energy sources with the distribution system. The specifications of all transformers and their ratings is listed in the table 2.

Table 2: Transformers data

| Transformer | T1 | T2 | T3 | T4_B | T5_G | T6_PV | T7_DC |
|---|---|---|---|---|---|---|---|
| Power (kVA) | 4000 | 1500 | 1500 | 55 | 3500 | 1000 | 15 |
| HV/LV | Yg69000/13800D1 | Y13800/220Y | Y13800/220 Y | D1900/220Y | Yg13800/2400D1 | Yg13800/250D1 | Y220/150Y |
| $R_{CC}$ (PU) | 0.015 | 0.03 | 0.03 | 0.003 | 0.015 | 0.0012 | 0.03 |
| $X_{CC}$ (PU) | 0.015 | 0.03 | 0.03 | 0.06 | 0.015 | 0.03 | 0.06 |

### e. Distribution line

The proposed system distributes the power at two different voltage levels i.e. at primary and secondary distribution level. For primary distribution level, the operating voltage is 13.8kv which is distributed by using 1/0 copper conductors. The unit resistance and reactance of the distribution

line is considered to be 0.394 ohm/km and 0.1168 ohm/km respectively, whereas the unit impedance is 0.411 ohm/km. for secondary distribution level, the operating voltage is 0.22 kV which is distributed by using 4/0 copper cables with the unit resistance and reactance of 0.198 ohm/km and 0.1089 ohm/km respectively and unit impedance of 0.227 ohm/km. Brief details of the line data is listed in the table 3.

Table 3: Line data

| Line | Resistance (ohm) | Reactance (ohm) | Distance (km) |
|---|---|---|---|
| L1_2 | 0.0297 | 0.016335 | 0.15 |
| L1_5 | 0.0396 | 0.02178 | 0.2 |
| L2_5 | 0.0297 | 0.016335 | 0.15 |
| L2_4 | 0.0792 | 0.04356 | 0.4 |
| L4_5 | 0.0792 | 0.04356 | 0.4 |
| L2_3 | 0.0792 | 0.04356 | 0.4 |
| L3_4 | 0.0198 | 0.01089 | 0.1 |
| L7_9 | 0.788 | 0.2336 | 2.0 |
| L6_11 | 2.364 | 0.7008 | 6.0 |
| L6_12 | 2.364 | 0.7008 | 6.0 |
| L6_13 | 1.182 | 0.3504 | 3.0 |
| L10_11 | 2.364 | 0.7008 | 6.0 |
| L13_14 | 1.182 | 0.3504 | 3.0 |
| L9_14 | 0.788 | 0.2336 | 2.0 |

### f. Loads

Various balance and linear unbalance loads are connected to the system and they are modeled as the constant impedances. There are few loads which are single phase connected to bus number 2 and 3, these single phase loads affects the symmetry of the current and voltage profile. The percentage between the maximum phase current deviation w.r.t. average load current gives the extent of unbalance load. The percentage unbalanced load is shown in equation (5) and (6). The various loads connected to the system is listed in table 4.

$$\%UL = \frac{\{|Ia-Iav|;|Ib-Iav|;|Ic-Iav|\}}{Iav} \quad (5)$$

$$Iav = \frac{Ia+Ib+Ic}{3} \quad (6)$$

where: Ia; Ib; Ic are the line RMS currents in phases a, b and c.

Table 4: Load data

| Bus no | Type of load | $L_{MAX}$ (kVA) | $L_{MIN}$ (kVA) | PF | %UL |
|---|---|---|---|---|---|
| 2 | UL | 40 | 12 | 0.9 | 13 |
| 3 | UL | 30 | 9 | 0.85 | 12.6 |
| 4 | L | 50 | 15 | 0.9 | |
| 9 | NL | 320 | 96 | 1 | |
| 10 | L | 800 | 240 | 0.8 | |
| 11 | L | 400 | 120 | 0.8 | |
| 12 | L | 800 | 240 | 0.8 | |
| 14 | L | 1600 | 480 | 0.8 | |

### g. Non-linear Loads

A non linear load, bridge rectifier is connected at Bus 9. The converter is operating at 4080 Hz carrier frequency in open loop PWM mode of operation with m-index of 0.8 with a DC load of 1084 Ω. Under minimum demand conditions, with unchanged PWM parameters, a DC load of 3615 Ω is substituted.

### h. DC micro-grid

The integration of a SST based DC micro-grid has been implemented in the proposed system. The SST provides enhanced control over voltage and frequency, improved load compensation, and a robust infrastructure for interfacing various DC and AC links. Additionally, the SST includes features similar to those of conventional power transformers (CPTs) in distribution grids, thereby enhancing the system's flexibility. Literature review presents various configurations for SSTs, which typically comprehend three distinct levels for power conversion well-suited for grid applications due to their endowment of two DC links. This versatility renders the SST suitable for multiple purposes within the electric grid. The block diagram of proposed system is shown in fig ure 2

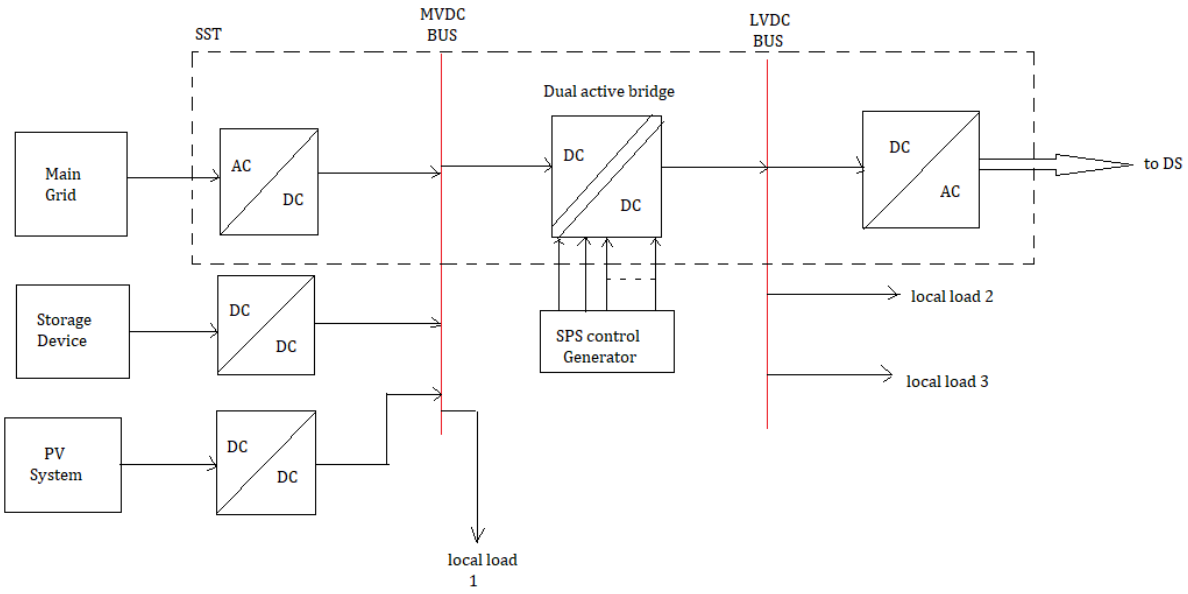


Figure 2: Block diagram of DCMG

The implemented DCMG comprises of one slack bus (main grid). Storage device and the PV system are connected to the MVDC bus of SST (800 VDC). Local DC loads are attached to both the buses and the interconnection link is provided at LVDC bus through dc to ac converter. DAB (dual active bridge) is used to provide interconnection between MVDC and LVDC buses. SPS control technique is used to provide firing pulses to the DAB. The implemented system specifications are mentioned in the table 5 below.

Table 5: DCMG component

| Component | Specification |
|---|---|
| Battery (Li-Ion) | 2-Ah , 700V |
| PV system | 40 KW |
| Loads | At MVDC- 20 KW DC<br>At LVDC- 5 KW DC |

## 3. POWER FLOW ANALYSIS

The hybrid system under consideration has been simulated using MATLAB/SIMULINK. Adaptive notch filter based on PLL is used for the calculation of phase angle at different buses. The PLL consist of auxiliary circuit which performs the extraction and subtraction of the phase angle of instantaneous values of waveforms of current and voltage in same phase. The subtraction outcomes the phase angle at the particular bus. [31] Shows the performance and design parameters of considered PLL.

The active (Pi) and reactive power (Qi) of the implemented system at various buses are calculated at fundamental frequency by using the power block. the magnitude of the peak values of input quantities |Vi| and |Ii| are calculated by using power block. After the information of input signals the output is calculated at fundamental frequency and is shown in (7), (8), and (9):

$$\varphi i = \angle \mathrm{Vi} - \angle \mathrm{Ii} \quad (7)$$

$$Pi = \frac{Vi}{\sqrt{2}}\frac{Ii}{\sqrt{2}}\cos(\varphi i) \quad (8)$$

$$Qi = \frac{Vi}{\sqrt{2}}\frac{Ii}{\sqrt{2}}\sin(\varphi i) \quad (9)$$

Where

Pi and Qi represents per phase active and reactive power respectively, |Vi| and |Ii| represents the peak voltage and peak current.$\varphi$i is the phase difference between voltage and current phasors of same phase. and i represents bus number.

The simulation of the system under consideration has been done in the MATLAB /Simulink environment. Table (6) and table (7) represents the load flow analysis for maximum and minimum demand scenario.

where

$P_g$ and $Q_g$ represent the real power and reactive power at generator bus.

$P_l$ and $Q_l$ represent the real power and reactive power at load bus.

$P_t$ and $Q_t$ represent the real power and reactive power at transfer bus.

Table 6: Load flow analysis for maximum demand

| Bus no. | $P_g$ (kW) | $Q_g$ (kVAR) | $P_l$ (kW) | $Q_l$ (Kvar) | $P_t$ (kW) | $Q_t$ (KVAr) | V (pu) | δ (deg) |
|---|---|---|---|---|---|---|---|---|
| 1 | 42.66 | 30.35 | | | | | 0.955 | -29.76 |
| 2 | | | | | 41.38 | 4.91 | 0.931 | -30.76 |
| 3 | | | 64.72 | 40.11 | 62.6 | 43.86 | 0.930 | -31.26 |
| 4 | | | | | 120.66 | 86.61 | 0.953 | -31.5 |
| 5 | | | | | 34.73 | 58.77 | 0.951 | -31.25 |
| 6 | | | | | 780 | 1095 | 0.966 | -30.31 |
| 7 | | | | | 554.6 | 356.2 | 0.971 | -30.72 |
| 8 | 690 | 450 | 0 | 0 | | | 0.975 | -60.84 |
| 9 | | | 327.3 | 38.23 | | | 0.966 | -30.67 |
| 10 | | | 572.4 | 427.2 | | | 0.940 | -29.81 |

| | | | | | | | | |
|---|---|---|---|---|---|---|---|---|
| 11 | | | 290.28 | 217.71 | | | 0.953 | -30.01 |
| 12 | | | 586.2 | 439.8 | | | 0.957 | -30.11 |
| 13 | 1810 | 1665 | 0 | 0 | | | 0.974 | -30.66 |
| 14 | | | 119.61 | 89.7 | 226.02 | 397.2 | 0.967 | -30.59 |

Table 7: Load flow analysis for minimum demand

| Bus no. | Pg (kW) | Qg (kVAR) | Pi (kW) | Qi (Kvar) | Pt (kW) | Qt (KVAr) | V (pu) | δ (deg) |
|---|---|---|---|---|---|---|---|---|
| 1 | 27.6 | 15.75 | | | | | 0.9567 | -31.27 |
| 2 | | | | | 12.64 | 5.77 | 0.959 | -31.28 |
| 3 | | | 21.1 | 13.09 | 25.47 | 14.43 | 0.967 | -31.14 |
| 4 | | | | | 50.3 | 25.74 | 0.979 | -31.14 |
| 5 | | | | | 51 | 26.79 | 0.983 | -31.24 |
| 6 | | | | | 471.2 | 346.1 | 0.980 | -30.31 |
| 7 | | | | | 89 | 84.4 | 0.98 | -30.25 |
| 8 | 150 | 49 | 0 | 0 | | | 0.98 | -60.23 |
| 9 | | | 110.2 | 0.69 | | | 0.98 | -30.28 |
| 10 | | | 183 | 135 | | | 0.97 | -30.15 |
| 11 | | | 92.1 | 69 | | | 0.97 | -30.21 |
| 12 | | | 184.8 | 138.6 | | | 0.98 | -30.24 |
| 13 | 92 | 74.1 | 0 | 0 | | | 0.99 | -30.29 |
| 14 | | | 372 | 279 | 21.84 | 84.6 | 0.98 | -30.30 |

## 4. SIMULATION ANALYSIS

The proposed model has been simulated and the simulation results have been analyzed and presented in this section. The power matrices for the efficiency and quality variable have also been presented. The proposed system is analyzed for two cases i.e. maximum and minimum demand case. Figure 3 shows the daily demand curve for the case under consideration. The daily demand curve is obtained be adding the hourly demands of every load.A slight difference can be seen between obtained nominal power of load and actual power consumption as loads are modeled as constant impedances. It is clear from the daily load curve that the minimum demand on the system is about 30% as compared to maximum demand. The DC micro-grid is also integrated with the already existing distribution system which utilizes the solid state transformer. Local DC loads are connected at the LVDC and HVDC side of the SST. The SST offers over voltage control frequency control, load compensation. Apart from the characteristics of conventional power transformer (CPT) it provides better infrastructure for interfacing various DC and AC link in a distribution grid. Solid state transformer consists of three different levels for power conversion is highly suitable for grid applications as it provides two DC links. Here the power flow results for

both the scenarios have been presented. so the use of SST helps in improving the flexibility of the system.

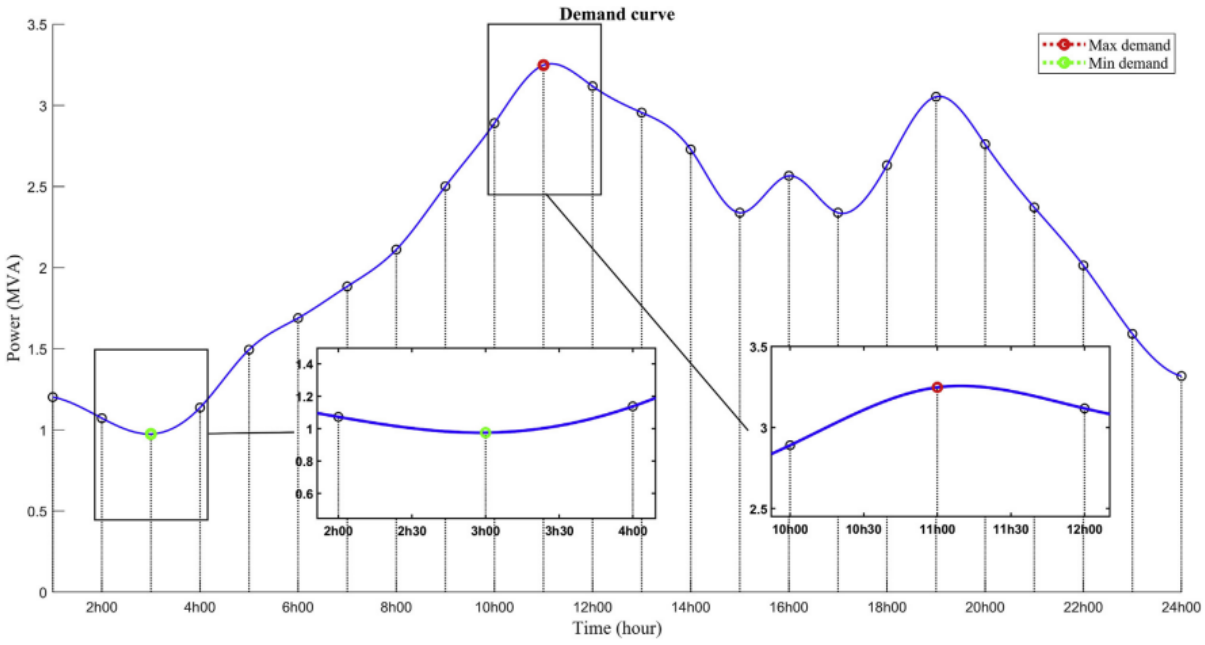


Figure 3: Daily demand curve

## I. Voltage profile

The simulation results of per phase voltage at different buses have been shown in figure 4 and figure 5. Figure 4 represents the voltage profile for and figure 5 represents the graph of voltage profile for peak demand situation with SST. The voltage graphs are per phase bases due to the presence of un-balance loads. It is clear from the results that the voltage is within the permissible limits for both the scenarios. There is small dip observed in the voltage curve at bus 2 and 3 i.e. in LV system in case of maximum demand scenario (SST is not introduced for this case). While voltage profile is improved with the introduction of SST that shows, SST can be used as power compensating device. The below equations show the calculation used in the given system. Equations below give the Average Deviation in the Voltage (ADVS) and Maximum Deviation in the Voltage(MVD) .

$$ADVS = \frac{\sum_{i=1}^{n} Vdi - Vi}{n} \quad (10)$$

$$MVD = \max_{(1<i<n)}(|Vd_i - V_i|) \quad (11)$$

where: n represents the number of buses in the Micro Grid;

Vi represents the real voltage at ith bus *(*p.u.);

Vdi represents the desired voltage at ith bus (p.u.);

ADVS signifies a figure of merit , need to be minimum for future optimization problem to improve voltage profiles.

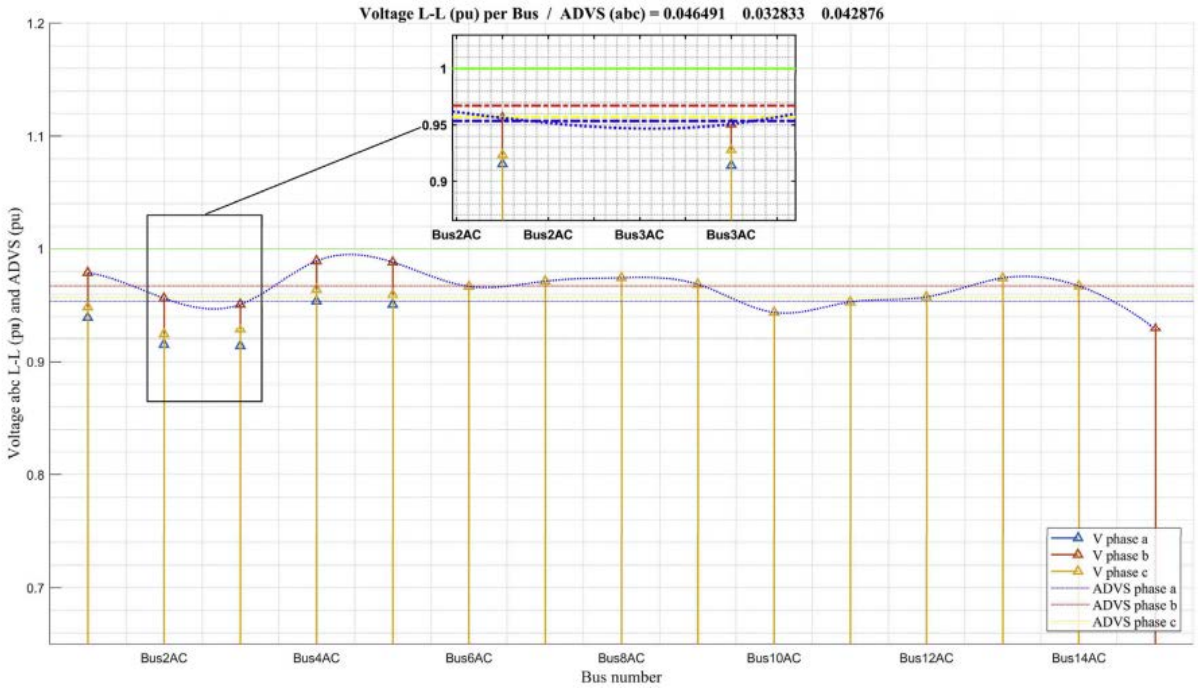


Figure 4: Voltage profile for Peak demand case without SST

Figure 4 shows the average deviation in the voltage at different buses for the proposed system in the peak demand situation, without SST based DC grid. The maximum deviation is in phase-a which is 0.047444.

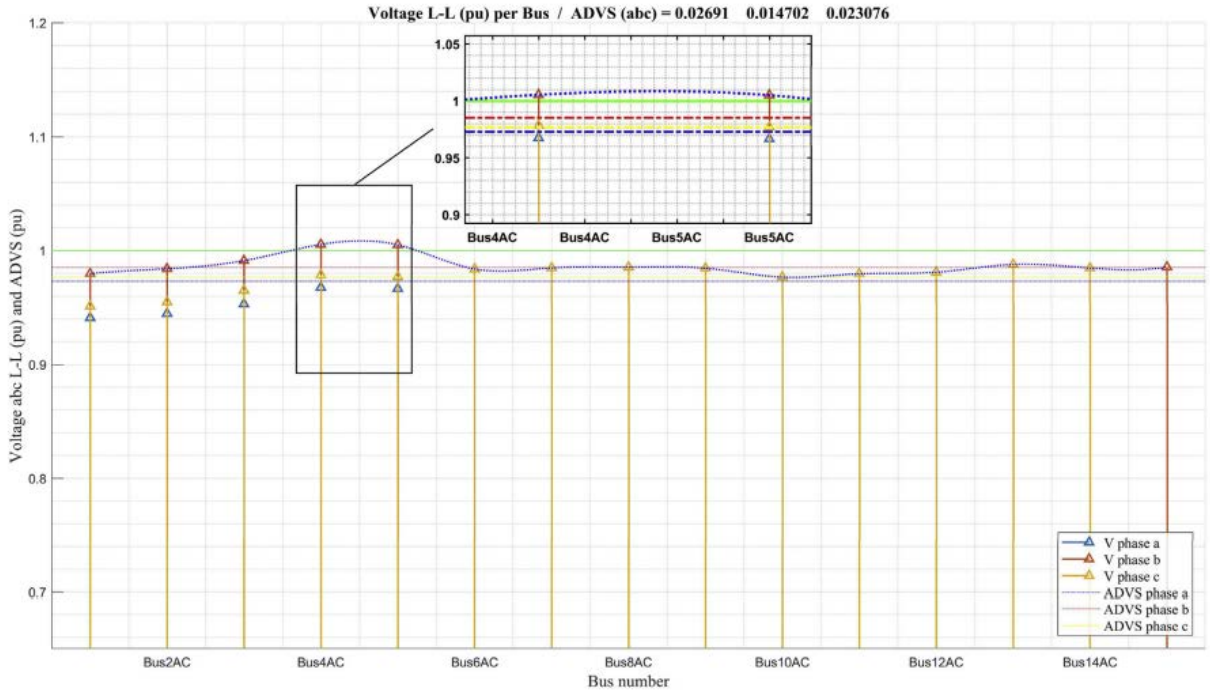


Figure 5: Voltage profile for peak demand case with SST

Figure 5 shows the average deviation in the voltage profile for individual phases at different buses for the SST based DC grid connected. It is clear from the results that average and the maximum deviation in the voltage are very low so it gives satisfactory operation of the system under consideration.

## II. Active Power Flow Balance

Figure 6 and 7 show the amount of active power at different buses. The positive values represents the amount of power consumes at the particular bus or the load power while the negative graphical representation shows the power generated or delivered at the given bus. There is negative power shown at but 14 which is actually transferred power contributed by diesel generator.

Figure 6 represents the maximum demand scenario while figure 7 represents the minimum demand scenario for the system under consideration. it is clear from the results that in case of maximum demand bus 1,2 8, 13 and DC bus supplies the demand while in case of minimum demand only bus 8 and 13 are supplying the demand while the DC micro-grid supplies the local loads.

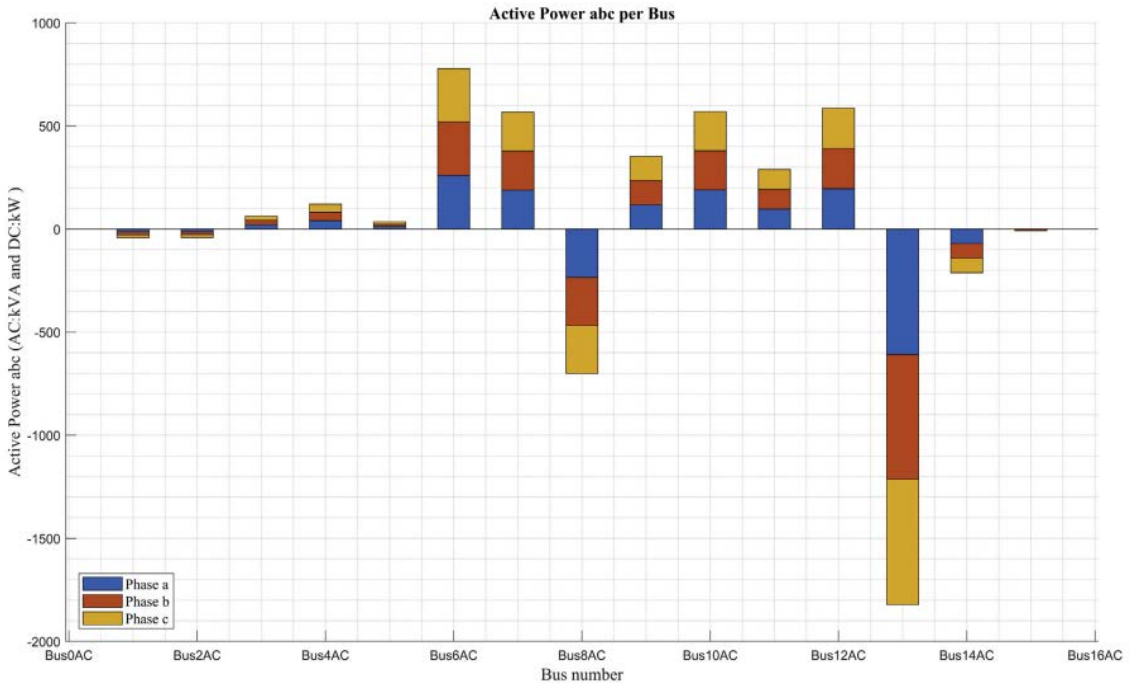


Figure 6: Active power flow for maximum demand case

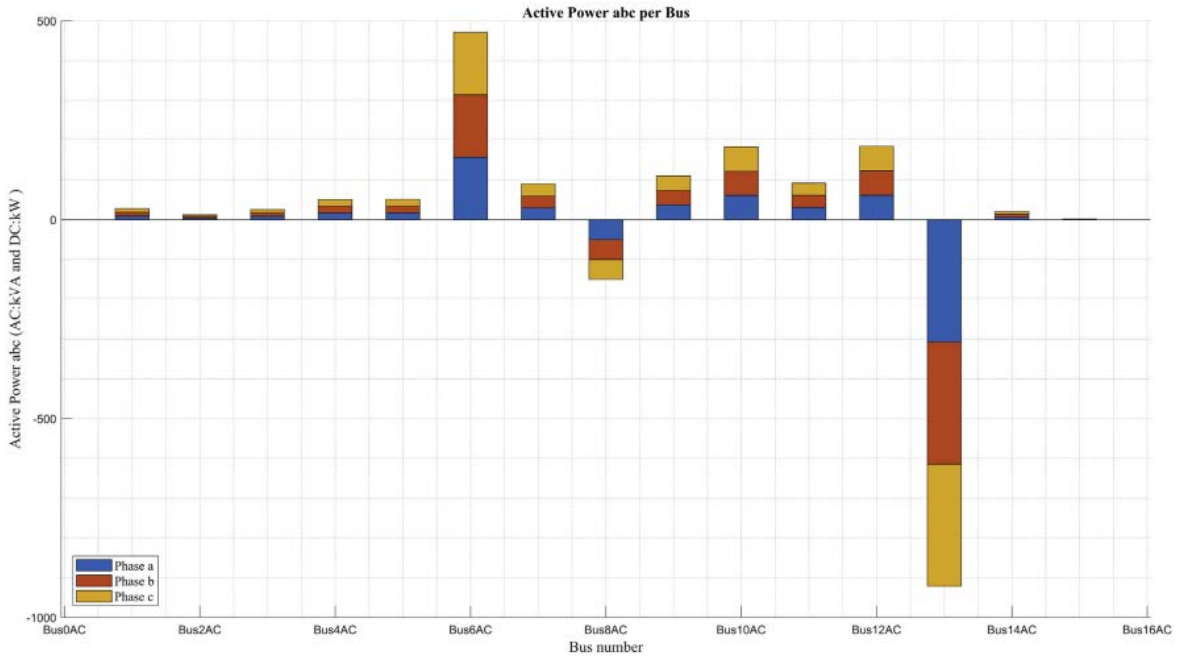


Figure 7: Active power flow for minimum demand case

## III. Reactive Power Flow Balance

Figure 8 and figure 9 shows the variation in the voltage and the reactive power flow per bus for the maximum and minimum demand scenarios respectively. Figures 8 and 9 clearly depicts t the relation between real and reactive power flow i.e. as there is increase in voltage profile ,the reactive power flow also increases. The positive and negative graphical peak shows the consumption and generation of reactive power at particular bus.

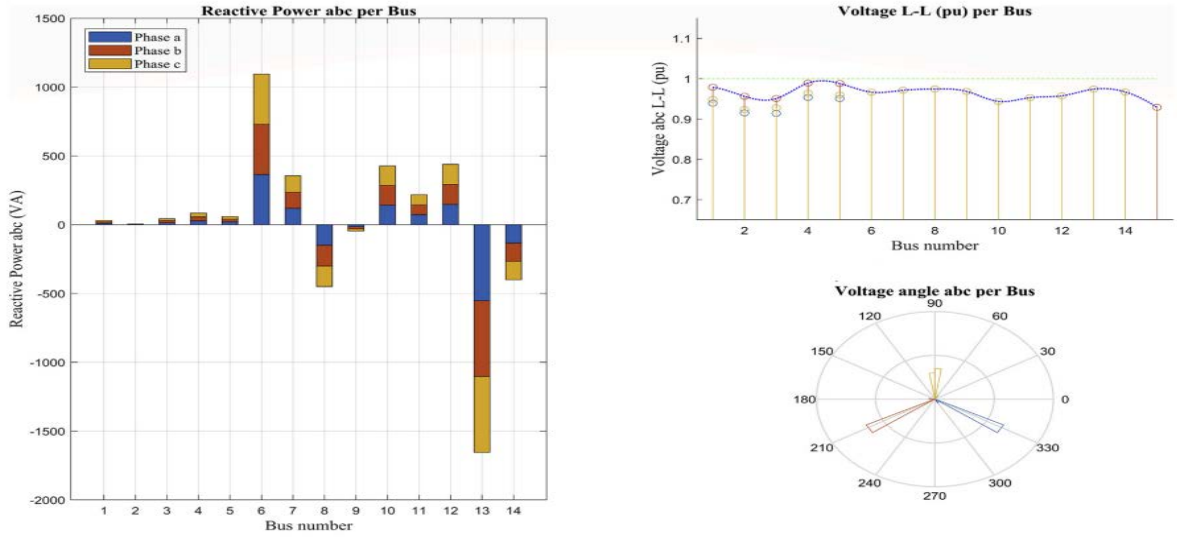


Figure 8: Reactive power flow and angle variation for maximum demand case

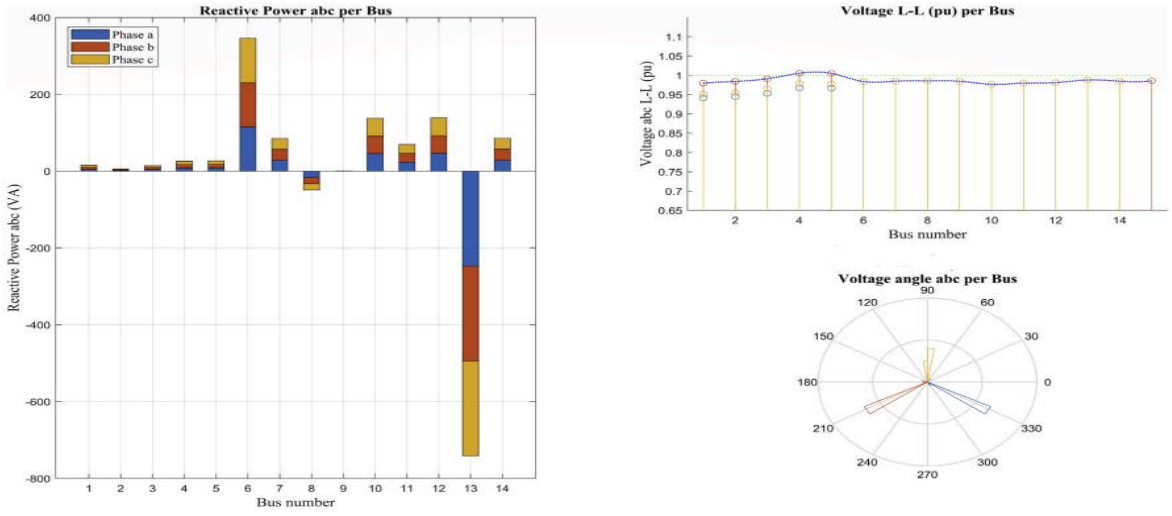


Figure 9: Reactive power flow and angle variation for minimum demand case

## IV. Loss analysis

The loss calculation has been done as per [32]. The equation shown below represents the per phase loss in the system under consideration

$$\Delta P_{a,b} = R_p * \sum_{i=1}^{n} |Ii, a, b|^2 + R_n * \sum_{i=1}^{n} |Ii, a, b|^2 \quad (12)$$

Where

$R_p$ = resistance of phase conductor

$R_n$ = resistance of neutral conductor.

$I_{i,a,b}$ = circulating line-b current during state of charge a in phase-i.

$\Delta P_{a,b}$ = power loss in line b during state of charge a.

Per phase losses of individual line for the proposed system is shown in figure 10 and figure 11 for the maximum demand and minimum demand respectively. In both the cases, the system line losses are more in LV system due to the presence of unbalance loads. In case of maximum demand scenario the highest loss is observed in line 7 which is around 9.8KW (in phase a), this is because of the flow of unbalance power in the line.

The non-uniformity in the power losses can be easily observed in the fig 10 and 11, this is because of the presence of unbalance loads in the system which in turn introduces single phase component in the system.

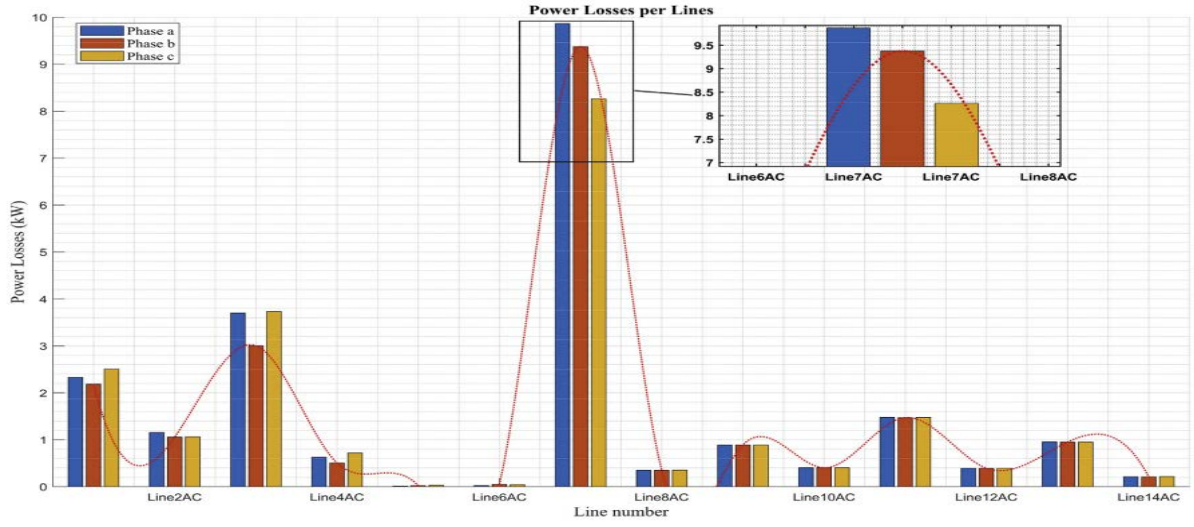


Figure 10: Per phase losses for maximum demand case

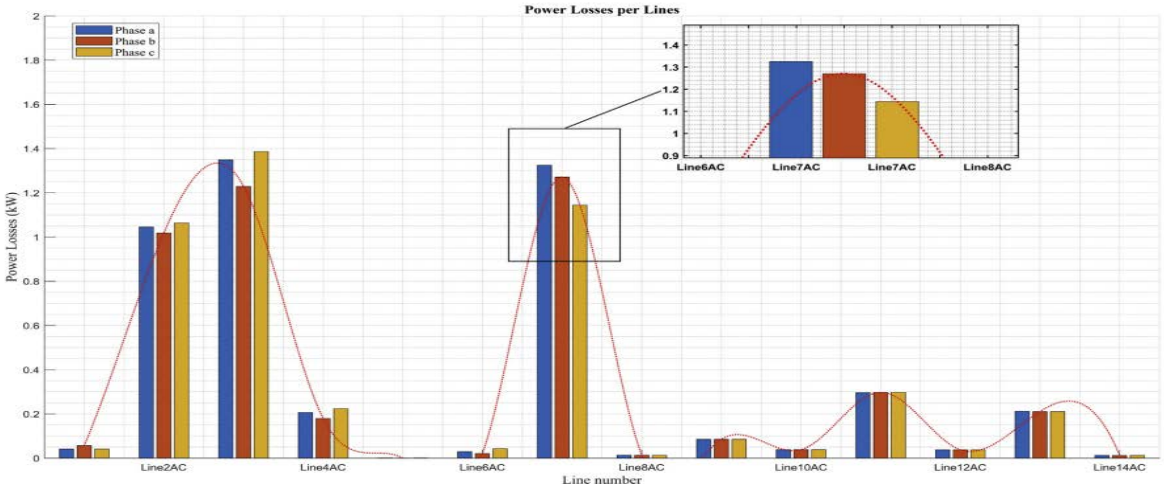


Figure 11: Per phase losses for minimum demand case

## V. Power factor analysis

Figure 12 and figure13 represents the power factor for the maximum demand and minimum demand respectively. The power factor in case of maximum demand at bus 2 and 9 is close to unity, bus 2 is connected to the DC micro grid through SST which improves the power factor. In the case of bus 9, power factor calculation depends on non-linear load using values specified in tables 8 and 9 for maximum demand and minimum demand.

Table 8: Maximum demand case

| Bus no. | Detail | Active power (KW) | Reactive power (KW) | Pf |
|---|---|---|---|---|
| 14 | Load | 1195.1 | 895 | O.8 |
| | Bus 14 | 226.04 | 397.1 | 0.49 |
| 9 | Bus 9 | 327.4 | 38.24 | 0.99 |

Table 9: Minimum demand case

| Bus no. | Detail | Active power (KW) | Reactive power (KW) | Pf |
|---|---|---|---|---|
| 14 | Load | 371 | 280 | O.8 |
| | Bus 14 | 21.80 | 84.9 | 0.09 |
| 9 | Bus 9 | 110.4 | 0.70 | 0.99 |

Bus 14 shows the poor performance when it comes to pf analysis this is because, this bus has been considered as transfer bus and the power flow for both the scenarios is mentioned in the table above. It is clear from the table that the flow of reactive power is more than the flow of active power transferred which results in low pf. Bus 5 is also a transfer bus that is why pf is low in case of maximum demand scenario as the transfer of reactive power is greater than the active power.

The p.f. of the proposed system is better in case of minimum demand than compared to maximum demand scenario. The reason behind this is reduction of reactive power demand in case of minimum demand scenario. Low pf is also observed at bus 6 due to the discontinuity in the output of PV system. The unpredictable weather condition can be a cause to losses in active power in case of PV system and also it does not generate power at night.As a result there is reduction in pf at bus 6.

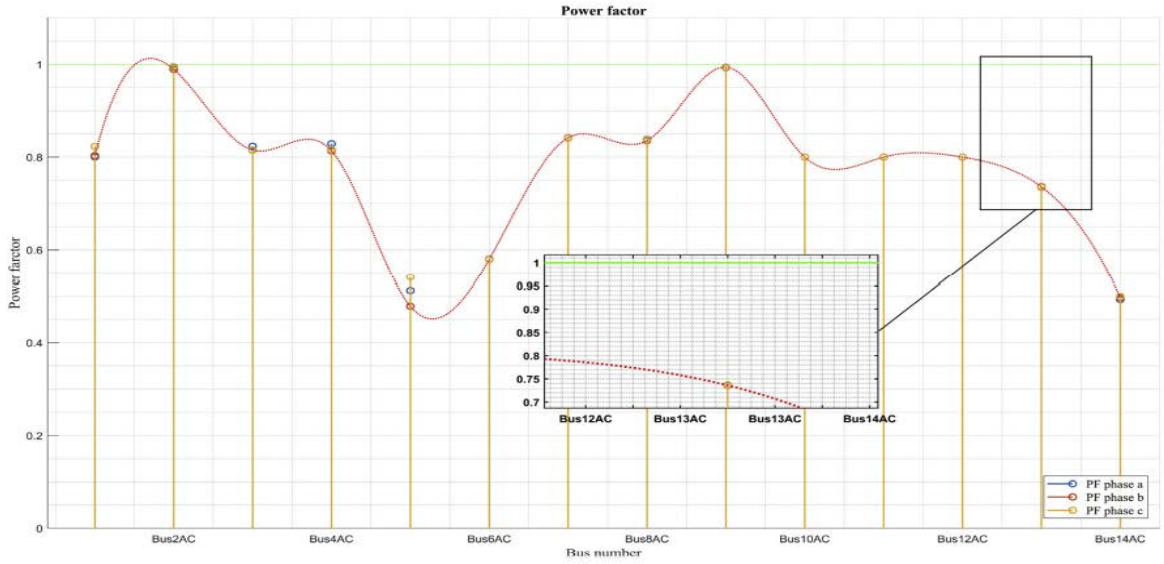


Figure 12: Per phase power factor maximum demand case

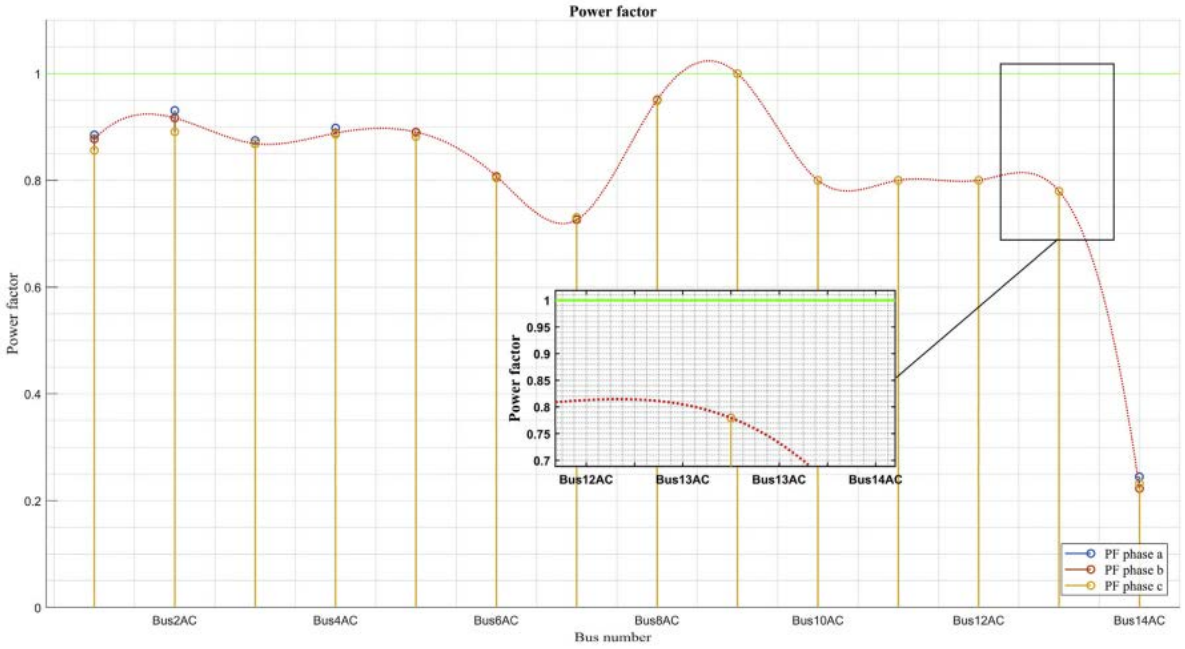


Figure 13: Per phase power factor maximum demand case

## VI. Calculation of Total harmonic distortion

Total Harmonic Distortion, THD is an important parameter for the power quality check in case of distribution system. THD is the measure of distortion present in the sine wave. Fig. 14 and 15 shows the THD index per phase of voltage waveform at individual bus for maximum and minimum demand cases respectively. Figure 14 and figure15 depicts that THD at each bus is within the permissible limits where h represents the highest harmonic order. THD is calculated by the equation

$$\%THD = \frac{\sqrt{(\sum_{i=2}^{h}(Vi,h)\text{^}2}}{Vi,1}*100 \qquad (13)$$

Where

$V_{i,h}$ = magnitude of ith node voltage corresponding to h-harmonic.

$V_{i,1}$ = fundamental harmonic component at node i.

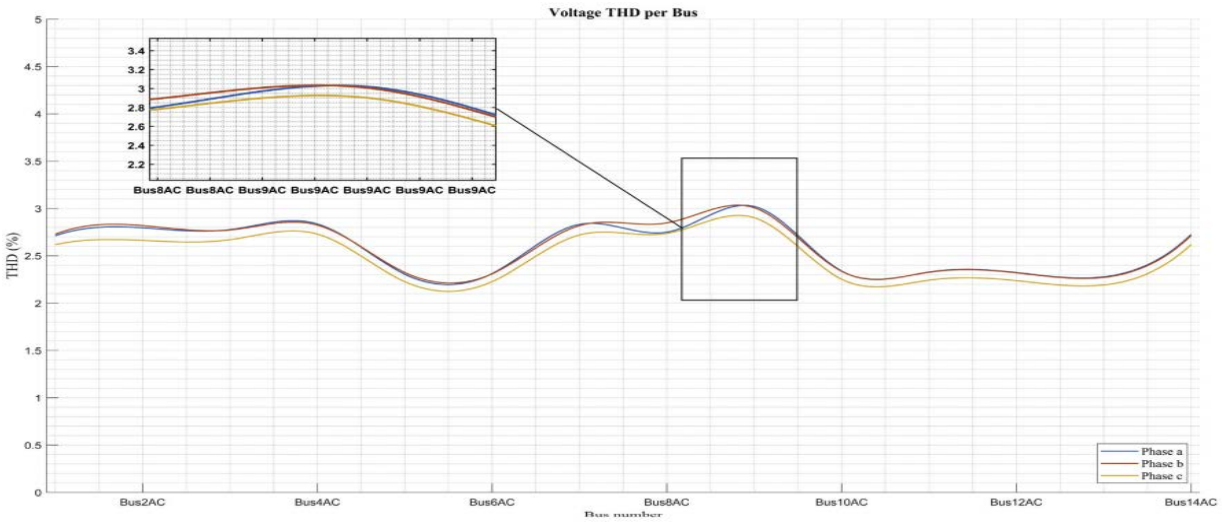


Figure 14: Total harmonic distortion in maximum demand

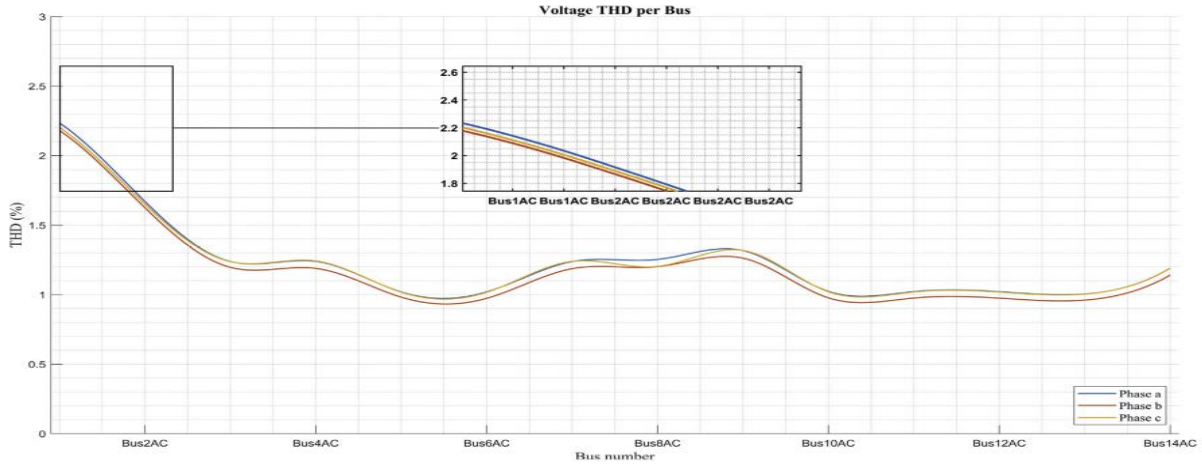


Figure 15: Total harmonic distortion in minimum demand case

## VII. SST based DC Micro-grid

The system under consideration consist of SST based DC MG. for the proposed MC micro-grid power flow analysis has been done for the different cases which are as follows

a. When PV generation is less than demand.
b. When PV generation is more than demand.

c. When PV is not linked to the system.

The proposed system is simulated for all three cases and power flow results have been analyzed.

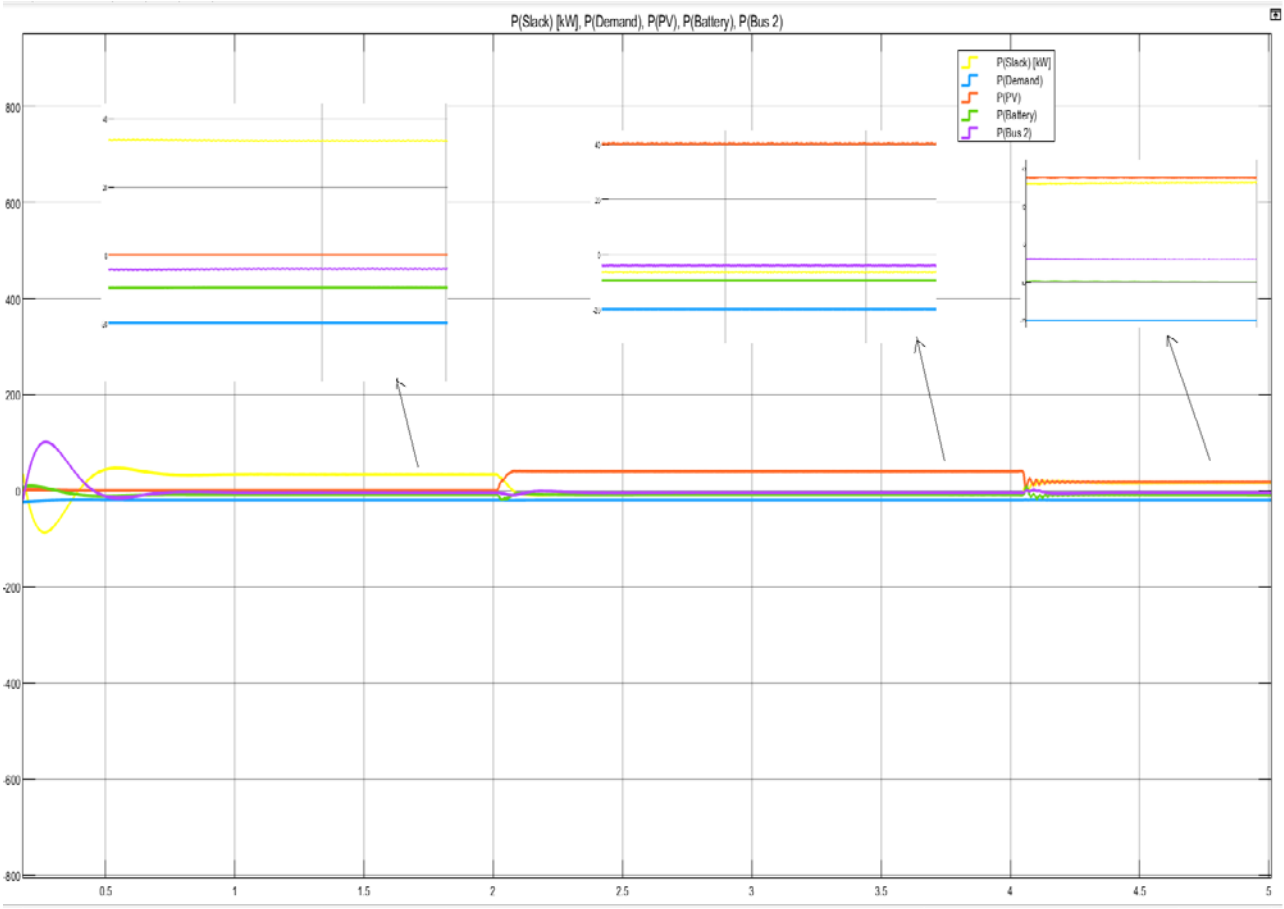


Figure 16: Power flow for DCMG

Table 10 shows the analysis of power flow for all three cases

Table 10: power flow results for DCMG

| Cases (time period in sec) | Condition | Power sharing (KW) |
|---|---|---|
| 1 (0<t<2.2) | PV= OFF | Demand = 24<br>PV = 0<br>Grid = 33<br>Battery = 9 (charging) |

| | | |
|---|---|---|
| 2 (2.2<t<4.2) | PV = ON ; $P_{PV} > P_{Demand}$ | Demand = 24<br>PV = 40<br>Grid = - 7<br>Battery = 9 (charging) |
| 3 (4.2<t<5) | PV = ON ; $P_{PV} < P_{Demand}$ | Demand = 24<br>PV = 17<br>Grid = 16<br>Battery = 9 (charging) |

In case 2 negative sign represents the reverse power flow i.e. excess power generated by PV system is going back to grid.

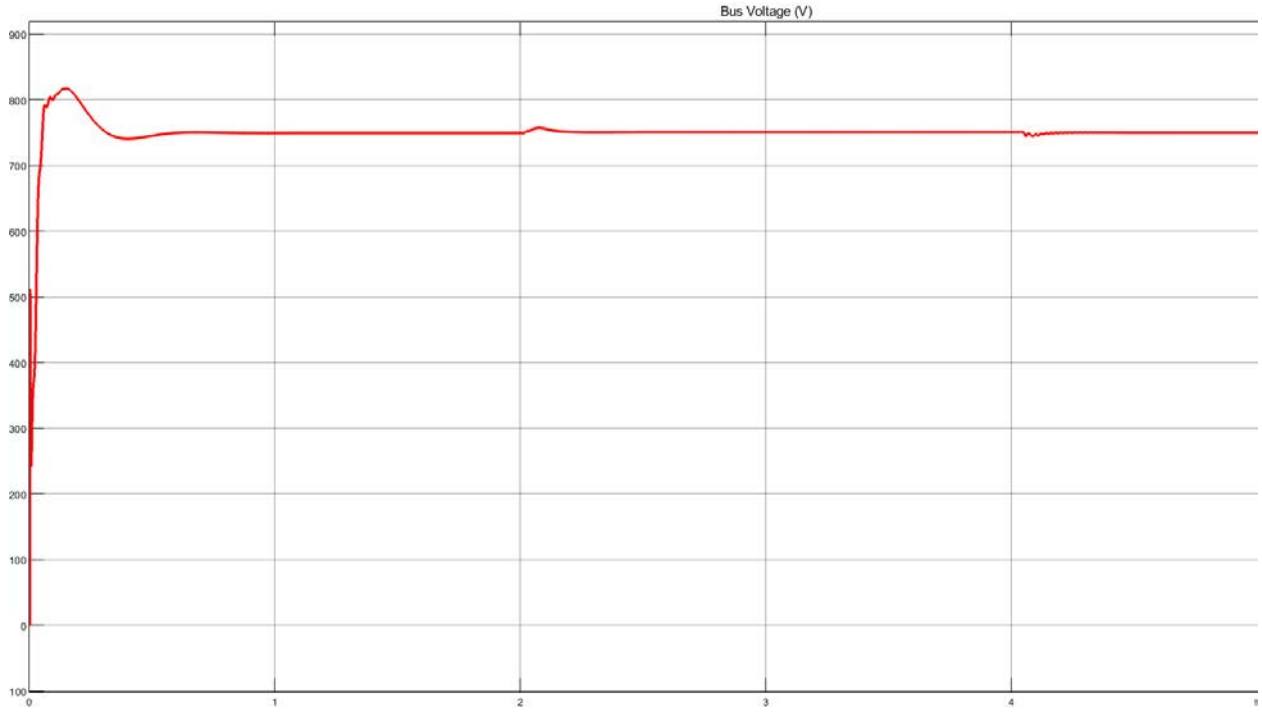


Figure 17: Common DC link voltage

Above figure represents the DC link voltage at medium voltage side of SST as all the power flow is through MVDC link only so it is important to maintain constant DC link voltage in spite of different working conditions. It can be clearly observed from the figure 17 that the MVDC link voltage is maintained constant for all the three cases.

## 5. CONCLUSION AND FUTURE SCOPE

In the presented work, a hybrid AC/DC 14-bus distribution system is proposed and simulated under maximum and minimum demand case. The proposed system consists of primary as well as

secondary distribution at 13.8 KV and 220 V respectively and the related data has been presented. The power flow results has been presented and discussed for both the cases. The the proposed system has been been simulated and analyzed considering different parameters like THD, power factor calculation, voltage profile at different buses and loss analysis with the help of measurement module at each bus. The results obtained forthe proposed system contributes the brief understanding of problem in terms of power quality that arises in MV and LV distribution system. The conflicts have also been discussed which arises because of discontinuity in PV output in case of power factor analysis.

In proposed system, SST based micro-grid is also been presented and integrated with already existing distribution system at low voltage side as there exist more dip in voltage profile in low voltage distribution system. The proposed DC micro-grid provides the smart solution for the grid interconnection due to the presence of two DC links. The SST also reduces the burden of DG converters and also provides the scope of DC line interconnection. So this study provides the better understanding of the HMG interconnected with distribution system. The proposed SST based DCMG enhances the system reliability and provide an attractive solution for grid interconnection and power flow management.

In future, the proposed system can be used to investigate the dynamic behavior of the micro-grid, performance of system in isolated condition. The DC link provided in DC MG can be extended for the purpose of electrical vehicle charging.

## 6. REFERENCES

[1] D.E. Olivares, A. et. Al., Trends in microgrid control, IEEE Trans. Smart Grid. 5 (2014) 1905–1919.

[2] H.A. Gabbar, Smart Energy Grid Engineering, Joe Hayton, Canada, 2017.

[3] A.K.G.K.G. Dimeas Aris, Tsikalakis, “Microgrids: Architectures and Control”, 2014.

[4] E. Planas, et, al., “AC and DC technology in microgrids: a review”, Renew. Sustain. Energy Rev. 43 (2015) 726–749.

[5] L. Jia, Y. Zhu, Y. Wang, Architecture design for new AC-DC hybrid micro-grid, in: IEEE 1st Int. Conf. Direct Curr. Microgrids, ICDCM 2015, 2015, pp. 113–118.

[6] S. Parhizi, H. Lotfi, A. Khodaei, S. Bahramirad, State of the art in research on microgrids: a review, IEEE Access 3 (2015) 890–925.

[7] F. Martin-Martínez, A. Sanchez-Miralles, M. Rivier, A literature review of Microgrids: a functional layer based classification, Renew. Sustain. Energy Rev. 62 (2016) 1133–1153.

[8] E. Hossain, E. Kabalci, R. Bayindir, R. Perez, Microgrid testbeds around the world: state of art, Energy Convers. Manag. 86 (2014) 132–153.

[9] G. Turner, J.P. Kelley, S. Member, C.L. Storm, D.A. Wetz, S. Member, W. Lee, Design and active control of a microgrid testbed, IEEE Trans. Smart Grid. 6 (2015) 73–81.

[10] M.S. Mahmoud, S.A. Hussain, M.A. Abido, Modeling and control of microgrid : an overview, J. Frankl. Inst. 351 (2014) 2822–2859.

[11] R.H. Lasseter, J.H. Eto, B. Schenkman, J. Stevens, H. Vollkommer, D. Klapp, E. Linton, H. Hurtado, J. Roy, CERTS microgrid laboratory test bed, IEEE Trans. Power Deliv. 26 (2011) 325–332.

[12] N.W.A. Lidula, A.D. Rajapakse, Microgrids research: a review of experimental microgrids and test systems, Renew. Sustain. Energy Rev. 15 (2011) 186–202.

[13] P. Piagi, R.H. Lasseter, Autonomous control of microgrids, in: 2006 IEEE Power Eng. Soc. Gen. Meet., 2006, p. 8.

[14] E. Commission, Smart Grid Projects Map: Organisations and Implementation Sites, 2018. http://ses.jrc.ec.europa.eu/.

[15] E.D.& E. RELIABILITY, Microgrid Portfolio of Activities, 2012. https://www.energy.gov/oe/services/technology-development/smart-grid/role-microgrids-helping-a dvance-nation-s-energy-syst-0.

[16] A. Kaur, J. Kaushal, P. Basak, A review on microgrid central controller, Renew. Sustain. Energy Rev. 55 (2016) 338–345.

[17] M.H. Andishgar, E. Gholipour, R. allah Hooshmand, An overview of control approaches of inverter-based microgrids in islanding mode of operation, Renew. Sustain. Energy Rev. 80 (2017) 1043–1060.

[18] Y. Yoldas¸, A. Onen, S.M. Muyeen, A.V. Vasilakos, _ I. Alan, Enhancing smart grid with microgrids: challenges and opportunities, Renew. Sustain. Energy Rev. 72 (2017) 205–214.

[19] J. John, F. Mwasilu, J. Lee, J. Jung, AC-microgrids versus DC-microgrids with distributed energy resources : a review, Renew. Sustain. Energy Rev. 24 (2013) 387–405.

[20] E. Unamuno, J.A. Barrena, Hybrid ac/dc microgrids - Part I: review and classification of topologies, Renew. Sustain. Energy Rev. 52 (2015) 1251–1259.

[21] E. Unamuno, J.A. Barrena, Hybrid ac/dc microgrids - Part II: review and classification of control strategies, Renew. Sustain. Energy Rev. 52 (2015) 1123–1134.

[22] S. Mirsaeidi, X. Dong, D.M. Said, Towards hybrid AC/DC microgrids: critical analysis and classification of protection strategies, Renew. Sustain. Energy Rev. 90 (2018) 97–103.

[23] A. Hirsch, Y. Parag, J. Guerrero, Microgrids: a review of technologies, key drivers, and outstanding issues, Renew. Sustain. Energy Rev. 90 (2018) 402–411.

[24] M.R. Amin, S. Aizam Zulkifli, A framework for selection of grid-inverter synchronisation unit: harmonics, phase-angle and frequency, Renew. Sustain. Energy Rev. 78 (2017) 210–219.

[25] R. Ortega, E. Figueres, G. Garcera, C.L. Trujillo, D. Velasco, Control techniques for reduction of the total harmonic distortion in voltage applied to a single-phase inverter with nonlinear loads: Review, Renew. Sustain. Energy Rev. 16 (2012) 1754–1761.

[26] P. Basak, S. Chowdhury, S. Halder Nee Dey, S.P. Chowdhury, A literature review on integration of distributed energy resources in the perspective of control, protection and stability of microgrid, Renew. Sustain. Energy Rev. 16 (2012) 5545–5556.

[27] U.B. Tayab, M.A. Bin Roslan, L.J. Hwai, M. Kashif, A review of droop control techniques for microgrid, Renew. Sustain. Energy Rev. 76 (2017) 717–727.

[28] M.R. Miveh, M.F. Rahmat, A.A. Ghadimi, M.W. Mustafa, Control techniques for three-phase four-leg voltage source inverters in autonomous microgrids: a review, Renew. Sustain. Energy Rev. 54 (2016) 1592–1610.

[29] M.T.L. Gayatri, A.M. Parimi, A.V. Pavan Kumar, A review of reactive power compensation techniques in microgrids, Renew. Sustain. Energy Rev. 81 (2018) 1030–1036.

[30] Z. Shuai, J. Fang, F. Ning, Z.J. Shen, Hierarchical structure and bus voltage control of DC microgrid, Renew. Sustain. Energy Rev. 82 (2018) 3670–3682.

[31] M. Karimi-Ghartemani, M.R. Iravani, A nonlinear adaptive filter for online signal analysis in power systems: Applications, IEEE Trans. Power Deliv. 17 (2002) 617–622.

[32] A. Aguila, D. Carrion, L. Ortiz, Analysis of power losses in the asymmetric construction of electric distribution systems, IEE Lat. Am. Trans. 13 (2015) 2190–2194.